Journal of Physics and Chemistry of Solids 81 (2015) 100–105

Contents lists available at ScienceDirect

Journal of Physics and Chemistry of Solids

journal homepage: www.elsevier.com/locate/jpcs

Enhanced thermoelectric performance of spark plasma sintered copper-deficient nanostructured copper selenide

Kriti Tyagi [a], Bhasker Gahtori [a], Sivaiah Bathula [a,b], M. Jayasimhadri [b], Niraj Kumar Singh [a], Sakshi Sharma [a], D. Haranath [a], A.K. Srivastava [a], Ajay Dhar [a,*]

[a] CSIR-Network of Institutes for Solar Energy, CSIR-National Physical Laboratory, Dr. K. S. Krishnan Road, New Delhi 110012, India
[b] Department of Applied Physics, Delhi Technological University, Delhi, India

ARTICLE INFO

Article history:
Received 3 November 2014
Received in revised form
23 January 2015
Accepted 31 January 2015
Available online 7 February 2015

Keywords:
Electron microscopy
Microstructure
Thermal conductivity
Electrical properties
Specific heat

ABSTRACT

We report the thermoelectric properties of nanostructured Cu-deficient Cu_2Se, which was *synthesized by high energy ball milling followed by spark plasma sintering. Our method obtained* a significant enhancement in the thermoelectric figure of merit (ZT), i.e., ~1.4 at 973 K, which was ~30% higher than its bulk counterpart. This enhancement in the thermoelectric performance was due mainly to a significant reduction in the lattice thermal conductivity, which was attributed to enhanced phonon scattering at various length scales by nanoscale defects as well as abundant nanograin boundaries. The nanoscale defects were characterized by transmission electron microscopy of the nanostructured $Cu_{2-x}Se$ samples, which formed the basis of the ZT enhancement.

1. Introduction

The conversion of waste heat into electrical energy without involving any moving parts in an eco-friendly manner using thermoelectric (TE) devices has received considerable attention in recent years [1]. During the last three decades, efforts have focused on the development of novel materials with high TE performance levels [2–4]. It is well known that the performance of a TE material is generally assessed based on its dimensionless figure of merit (ZT) $= S^2\sigma T/\kappa$, where S, σ, T, and κ are the Seebeck coefficient, electrical conductivity, absolute temperature, and thermal conductivity, respectively [4]. Furthermore, the total thermal conductivity (κ) is the sum of the lattice thermal conductivity (κ_l) due to phonons and the electronic thermal conductivity (κ_e) due to charge carriers [5, 6] travelling through the lattice. However, the simultaneous optimization of these physical parameters to obtain a high ZT is difficult because they are inter-dependent and a change in any one of these parameters affects the others adversely.

Several strategies have been employed to enhance the ZT of TE materials, which have focused on optimizing the power factor ($S^2\sigma$) through controlled doping [7,8], reducing the thermal conductivity using solid-solution alloying [9], or employing the nanostructuring approach [10]. Indeed, remarkable progress has been made in improving the ZT for several TE materials using the latter approach [11,12]. Quantum confinement effects induced by nanostructuring tend to enhance the Seebeck coefficient while the presence of numerous nanoscale interfaces tend to scatter phonons more effectively than charge carriers, thereby reducing the thermal conductivity significantly [13] and increasing the ZT considerably.

Various TE material nanostructures such as super-lattices [13–15], nanowires [16], and nanocomposites [17–20] have been developed to improve the ZT appreciably. However, the high ZT in these nanostructures is not very useful in practice because these fabrication processes are expensive and their power handling capacity is limited. By contrast, bulk nanostructured materials [21] fabricated using the conventional powder metallurgical technique [22] can be produced economically in large quantities and in a form that is compatible with commercially available devices.

Among the existing TE materials, Cu_2Se-based materials are the most intriguing compounds because they exhibit a high TE performance due to the liquid-like behavior of Cu ions around the Se sub-lattice at high temperatures [23]. Stoichiometric and non-stoichiometric $Cu_{2-x}Se$ exists in different crystallographic forms such as cubic [24], monoclinic [25], orthorhombic, and tetragonal configurations [26, 27]. However, it is well known that stoichiometric Cu_2Se becomes non-stoichiometric at high operating temperatures, thereby limiting its usage in actual device applications [23]. In the current study, we report the synthesis and transport

---

[*] Corresponding author. Fax: +91 11 4560 9310.
E-mail address: adhar@nplindia.org (A. Dhar).

http://dx.doi.org/10.1016/j.jpcs.2015.01.018
0022-3697/

properties of copper-deficient Cu_2Se, which is stable up to its operating temperature (973 K), where its ZT exhibits the maximum value.

Liu *et al.* [23] reported a ZT of ~1.1 at 1000 K for bulk $Cu_{1.98}Se$. Later, Xiao *et al.* [28] reported the phase transition and TE properties of $Cu_{2-x}Se$ synthesized by melt-quenching and using the spark plasma sintering (SPS) technique, which yielded a ZT value of ~0.38 at 750 K. However, there are no previous reports of nanostructured $Cu_{2-x}Se$. Thus, to optimize the electrical conductivity by creating Cu vacancies and the thermal conductivity by nanostructuring $Cu_{2-x}Se$, we prepared several $Cu_{2-x}Se$ samples with various Cu concentrations and obtained the optimal TE properties in nanostructured $Cu_{1.98}Se$. We observed that the enhancement of the ZT was primarily due to a drastic reduction in κ because nanostructuring yielded abundant grain boundaries and microstructural defects, which acted as scattering centers for phonons at various wavelength scales. Therefore, our nanostructuring approach for producing $Cu_{1.98}Se$ obtained a ZT value of ~1.4 at 973 K, which is ~30% higher than its bulk counterpart.

2. Experimental procedure

Cu (99.99%, *Alfa Aesar*) and Se (99.99%, *Alfa Aesar*) powders were milled in a ball mill setup (Fritsch, Pulverisette-5) for an optimized time period of ~50 h. The containers used for the ball-mill and the milling media were made of stainless steel. The ball: powder ratio was optimized at 20:1 by weight. Milling was performed in an argon atmosphere at a speed of 400 rpm. In order to prevent re-welding and to promote fracturing of the powder particles, 2 wt% of stearic acid was added as a process control agent. Prior to sintering, the nanostructured alloy powders were processed in a glove box (Mbraun, *MB20*) to avoid oxidation and other atmospheric contamination. Phase identification and crystallite size measurements were performed by X-ray powder diffraction (XRD) (Rigaku, *MiniFlexII*). The stoichiometric bulk $Cu_{1.98}Se$ was synthesized using a vacuum melting process with high-purity Cu and Se powders, which were ground thoroughly in a glove box under a high-purity argon atmosphere. The powders were then made into pellets and vacuum-sealed (10^{-4} Torr) in quartz tubes. The sealed quartz ampoules were placed in a box furnace, heat-treated at 800 °C for 96 h, and then cooled naturally to room temperature (~25 °C). Next, the nanostructured and bulk alloy powders were consolidated and sintered under vacuum (~ 4 Pa) using SPS (SPS Syntex, *725*) at a pressure of 60 MPa at 600 °C, with a heating rate of 300 °C/min and a soaking time of ~4 min, respectively, where we employed a 12.7-mm diameter graphite die and punches. The actual compositions of the melt-processed bulk and nanostructured samples were determined using flame atomic absorption spectrometry (Analytik Jena,Vario-6), where both of the samples exhibited almost the same stoichiometry as the starting composition, i.e., $Cu_{1.96}Se$ for bulk samples and $Cu_{1.97}Se$ for nanostructured samples. The density was measured using the conventional Archimedes principle. Electron microscopy experiments were performed with a high-resolution transmission electron microscope (HRTEM) (Tecnai G2 F30 STWIN) at an electron accelerating voltage of 300 kV using the electron source as a field emission gun. HRTEM was used to study the morphology, interfacial microstructural characteristics, and crystallographic orientation of the as-sintered bulk and nanostructured samples. Specific heat measurements were obtained using a differential scanning calorimeter (DSC) (Mettler Toledo, *DSC842*). The thermal diffusivity was measured using polished sample discs with a diameter of 12.7 mm and a thickness of 3 mm in a laser flash system (Linseis, *LFA 1023*). The thermal conductivity was calculated as the product of the thermal diffusivity, specific heat, and volume density. The Seebeck coefficient and resistivity were measured using a commercial system (Ulvac, *ZEM 3*) with polished sample bars that measured $\sim 3 \times 3 \times 11\ mm^3$. The accuracies of the measurements were: ±6% for thermal diffusivity, ± 10% for electrical conductivity, ±7% for the Seebeck coefficient, ±8% for specific heat, and ±0.5% for density.

3. Results and discussion

In this study, we performed phase transition and thermal stability analyses of $Cu_{2-x}Se$ with different Cu compositions based on DSC measurements. Fig. 1 shows clearly that the phase transition temperature decreased as the Cu concentration in $Cu_{2-x}Se$ also decreased. A similar behavior was observed by other researchers using a Cu-deficient bulk $Cu_{1.98}Se$ material [28]. The XRD patterns of the bulk and nanostructured $Cu_{1.98}Se$ samples in Fig. 2 show that there was significant peak broadening in the nanostructured sample compared with its bulk counterpart, which was due primarily to its nanostructured grain features. The crystallite size was evaluated based on the XRD data after accounting for instrumental broadening and we used the Williamson-Hall method to consider the lattice strain [29,30]. The average crystallite size of the nanostructured $Cu_{1.98}Se$ sample after SPS was found to be ~12 nm. The XRD patterns that we obtained for the $Cu_{1.98}Se$ samples were compared with previously reported data for $Cu_{1.98}Se$ [23,28], which confirmed the phase purity.

Our detailed microstructural characterization of the nanostructured and bulk samples of $Cu_{1.98}Se$ elucidated several interesting features in real and reciprocal space. In the nanostructured alloy, we observed a uniformly distributed ultra-fine microstructure at lower magnification, as shown in Fig. 3(a), where individual grains with a boundary length of about 3–6 nm are clearly visible (indicated by the dotted line between grains A and B in Fig. 3(a)). The individual grains sometimes exhibited a mottled contrast due to the strain in the microstructure (A and B in Fig. 3(a)). There were significant Moiré fringes in the matrix of the microstructure, presumably due to the overlapping of tiny nanocrystals. As an illustrative example, a region with Moiré fringes is indicated as C in Fig. 3(a). The magnified view of an individual grain (A) in Fig. 3(b) shows that the entire nanocrystal comprised planes of *hkl*: 220, where the inter-planar spacing was 0.21 nm. At the interface of grains A and B (the region indicated by the dotted line in Fig. 3(a)), the boundary was clearly distinct with

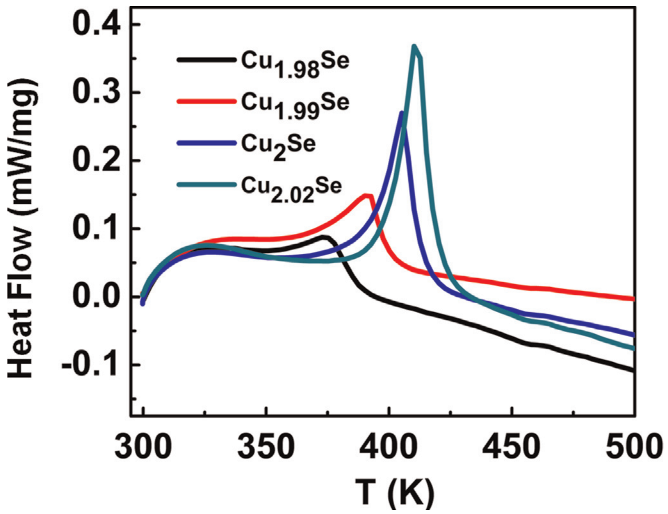

Fig. 1. Differential scanning calorimetry measurements of nanostructured $Cu_{2-x}Se$ with different Cu compositions.